Cell Calcium 77 (2019) 68–76

Contents lists available at ScienceDirect

Cell Calcium

journal homepage: www.elsevier.com/locate/ceca

Regulation of inositol 1,4,5-trisphosphate-induced Ca^{2+} release from the endoplasmic reticulum by AMP-activated kinase modulators

Jessica Arias-del-Val[a], Jaime Santo-Domingo[b], Paloma García-Casas[a], Pilar Alvarez-Illera[a], Antonio Núñez Galindo[b], Andreas Wiederkehr[b], Rosalba I. Fonteriz[a], Mayte Montero[a], Javier Alvarez[a,*]

[a] Institute of Biology and Molecular Genetics (IBGM), Department of Biochemistry and Molecular Biology and Physiology, Faculty of Medicine, University of Valladolid and CSIC, Ramón y Cajal, 7, E-47005 Valladolid, Spain
[b] Mitochondrial Function and Proteomics, Nestle Institute of Health Science S.A. EPFL Innovation Park, 1015, Lausanne, Switzerland

ARTICLE INFO

Keywords:
AMPK
Inositol-1,4,5-trisphosphate receptor
Ca^{2+} signaling
Endoplasmic reticulum
A769662
Dorsomorphin

ABSTRACT

The 5' AMP-activated protein kinase (AMPK) is a nutrient-sensitive kinase that plays a key role in the control of cellular energy metabolism. We have explored here the relationship between AMPK and Ca^{2+} signaling by looking at the effect of an AMPK activator (A769662) and an AMPK inhibitor (dorsomorphin) on histamine-induced Ca^{2+}-release from the endoplasmic reticulum (ER) in HeLa cells. Our data show that incubation with A769662 (EC_{50} = 29 μM) inhibited histamine-induced Ca^{2+}-release from the ER in intact cells, as well as inositol-1,4,5-trisphosphate (IP_3)-induced Ca^{2+} release in permeabilized cells. On the contrary, dorsomorphin (EC_{50} = 0.4 μM) activated both histamine and IP_3-induced Ca^{2+}-release and reversed the effect of A769662. These results suggest a direct effect of AMPK regulation on IP_3 receptor (IP_3R) function. A phosphoproteomic study did not reveal changes in IP_3R phosphorylation, but showed significant changes in phosphorylation of proteins placed upstream in the IP_3R interactome and in several proteins related with Ca^{2+} metabolism, which could be candidates to mediate the effects observed. In conclusion, our data suggest that AMPK negatively regulates IP_3R. This effect constitutes a novel and very important link between Ca^{2+} signaling and the AMPK pathway.

1. Introduction

5' AMP-activated protein kinase (AMPK) plays a key role in cellular energy homeostasis. AMPK is a sensor of adenine nucleotides that is activated when cellular energy is low and tries to restore energy balance by activating ATP-producing catabolic pathways and inhibiting ATP-consuming anabolic pathways. In addition, recent studies suggest that it may be able to sense glucose levels directly by a non-canonical mechanism, that is, independently of changes in adenine nucleotides [1]. Activation of AMPK leads to modulation of several metabolic pathways, including stimulation of hepatic fatty acid oxidation and ketogenesis, inhibition of cholesterol synthesis, lipogenesis, and triglyceride synthesis, inhibition of adipocyte lipolysis and lipogenesis, stimulation of skeletal muscle fatty acid oxidation and muscle glucose uptake [2].

The effects of AMPK on energy metabolism are in part mediated by inhibition of the mTOR pathway. Together with insulin signaling, AMPK and mTOR are the key nutrient sensitive pathways that adapt metabolism to the nutrient intake. Moreover, these pathways appear to be critical effectors of aging, mTOR on the pro-aging side and AMPK on the pro-longevity side [3,4]. Understanding the regulation of these pathways is therefore essential to uncover the relationship between metabolism and aging, and to find new approaches to slow the aging process.

AMPK activation can be triggered by phosphorylation of T172 in the α-subunit or by AMP/ADP binding to the γ-subunit. ATP competitively inhibits the binding of both AMP and ADP to the γ-subunit, and thus AMPK behaves as a sensor of AMP/ATP or ADP/ATP ratios. Phosphorylation at T172 of the AMPK α-subunit can be carried out by several kinases, one of them the calcium-/calmodulin-dependent kinase

Abbreviations: AMPK, 5' AMP-activated protein kinase; ER, endoplasmic reticulum; MAMs, Mitochondrial Associated ER Membranes; IP_3, inositol-1,4,5-trisphosphate; IP_3R, IP_3 receptor; MCU, mitochondrial Ca^{2+} uniporters; BMPR, bone morphogenetic protein receptors

* Corresponding author at: Institute of Biology and Molecular Genetics (IBGM), Department of Biochemistry and Mol. Biol. and Physiology, Faculty of Medicine, Ramón y Cajal, 7, E-47005 Valladolid, Spain.
E-mail address: jalvarez@ibgm.uva.es (J. Alvarez).

https://doi.org/10.1016/j.ceca.2018.12.004
Received 3 September 2018; Received in revised form 10 December 2018; Accepted 10 December 2018
Available online 11 December 2018
0143-4160/

kinase 2 (CaMKK2). The interaction of CaMKK2 with AMPK only involves the α and β subunits of AMPK. Using this mechanism, AMPK becomes activated by changes in calcium levels but not by changes in AMP/ATP or ADP/ATP ratios [5,6].

There is considerable evidence for the role of Ca^{2+} signaling in the modulation of the nutrient-sensitive pathways, although the mechanisms are not completely known [7]. Regulation of mTOR and AMPK by Ca^{2+} may take place at several levels. First, activation by Ca^{2+} of CaMKK2 leads to AMPK activation, which in turn inhibits mTOR. Using this pathway, Ca^{2+} indirectly inhibits mTOR [8]. On the other hand, there is also evidence that Ca^{2+} can directly activate mTOR. It has been described that amino acids added to nutrient-deficient cells induce an increase in cytosolic Ca^{2+} that activates mTOR through the binding of the Ca^{2+}-calmodulin complex to a class III phosphatidylinositol 3-kinase necessary for the activation of mTOR [9]. Likewise, it has been described that muscle hypertrophy induced by training is mediated by the activation of Ca^{2+} channels of the TRPV1 type, which produce Ca^{2+} entry into the cytosol. An increase in cytosolic Ca^{2+} would produce a direct and immediate activation of mTOR, responsible for initiating the hypertrophy process [10]. In these cases, the increase in cytosolic Ca^{2+} would have an activating effect on mTOR.

One of the key mediators of Ca^{2+} fluxes linked to the activity of mTOR and AMPK is the inositol triphosphate receptor (IP_3R), which releases Ca^{2+} from the endoplasmic reticulum (ER) and is also responsible for transferring Ca^{2+} from the ER to the mitochondria through close contacts between the organelles. These contacts, called Mitochondrial Associated ER Membranes (MAMs), contain both IP_3R and mitochondrial Ca^{2+} uptake channels, the so-called mitochondrial Ca^{2+} uniporters (MCU). In addition to IP_3R and MCU, it has been shown that mTORC2 is also in MAM, controls its integrity and is able to activate AKT kinase, which finally phosphorylates and inhibits IP_3R [11]. On the other hand, it has also been reported that mTOR is able to directly phosphorylate and activate IP_3R [12–14]. The resulting increased Ca^{2+} transfer between ER and mitochondria would lead to increased ATP production and subsequent AMPK inhibition [15].

In turn, variations in the activity of the IP_3R can alter the nutrient sensitive pathways. When the release of Ca^{2+} mediated by IP_3R is reduced, Ca^{2+} entry to the mitochondria decreases and this reduces the rate of ATP synthesis. This energy deficit activates AMPK, which in turn inhibits mTOR. In this way, a deficient Ca^{2+} transfer between ER and mitochondria may lead to mTOR inhibition [8] and may significantly impair survival of tumorigenic cells [16]. Finally, it has also been described that mTOR is capable of activating the store-operated Ca^{2+} entry pathway (SOCE), via an increase in the expression of the STIM1 / Orai1 proteins responsible for this pathway [17].

In summary, it has been described in the literature that Ca^{2+} homeostasis and nutrient-sensitive pathways have multiple interactions, but the mechanisms and sense of interaction are not yet clear. We have studied the effect of AMPK modulators on intracellular Ca^{2+} signaling in cytosol, mitochondria and endoplasmic reticulum. Our data show that the AMPK activator A769662 inhibits Ca^{2+} release from the endoplasmic reticulum through the IP_3R, while the AMPK inhibitor dorsomorphin enhances IP_3-induced Ca^{2+} release. This suggests that AMPK, besides being activated by a Ca^{2+}-sensitive mechanism (via CaMKK2), it may also directly modulate Ca^{2+} signaling at the IP_3R level.

2. Methods

2.1. Cell culture and targeted aequorin expression

HeLa cells were grown in Dulbecco's modified Eagle's medium supplemented with 10% fetal calf serum, 100 i.u. ml-1 penicillin and 100 i.u. ml-1 streptomycin. The constructs for aequorin targeted to the cytosol, mutated aequorin targeted to the mitochondria and double-mutated aequorin targeted to either mitochondria or the endoplasmic reticulum (ER) have been described previously [18–20]. Transfections were carried out using Metafectene (Biontex, Munich, Germany).

2.2. $[Ca^{2+}]_C$, $[Ca^{2+}]_M$ and $[Ca^{2+}]_{ER}$ measurements with aequorin

HeLa cells were plated onto 13 mm round coverslips and transfected with the corresponding plasmid. For aequorin reconstitution, HeLa cells were incubated for 1–2 h at room temperature in standard medium (145 mM NaCl, 5 mM KCl, 1 mM $MgCl_2$, 1 mM $CaCl_2$, 10 mM glucose, and 10 mM HEPES, pH 7.4) with 1 μM of wild-type coelenterazine or 1 μM of coelenterazine i (for $[Ca^{2+}]_{ER}$ measurements with double mutated aequorin in intact cells). After reconstitution, cells were placed in the perfusion chamber of a purpose-built luminometer and perfused with external medium prior to the stimuli.

For the $[Ca^{2+}]_{ER}$ measurements in permeabilized cells, $[Ca^{2+}]_{ER}$ was reduced before reconstitution by incubating the cells for 10 min with the sarcoplasmic and endoplasmic reticulum Ca^{2+}-ATPase inhibitor 2,5-di-tert-buthyl-benzohydroquinone (BHQ) 10μM in standard medium supplemented with 0.5 mM EGTA. Cells were then washed and incubated for 1 h at room temperature in the same medium with 1μM of wild-type coelenterazine. Then, the coverslip was placed in the perfusion chamber of the luminometer, and standard medium containing 0.5 mM EGTA was perfused for 5 min, followed by 1 min of intracellular medium (130 mM KCl, 10 mM NaCl, 1 mM $MgCl_2$, 1 mM potassium phosphate, 0.5 mM EGTA, 1 mM ATP, 20 μM ADP, 10 mM L-malate, 10 mM glutamate, 20 mM Hepes, pH 7) containing 50 μM digitonin. Then, intracellular medium without digitonin was perfused for 5 min, followed by a 100 nM $[Ca^{2+}]$ buffer prepared in intracellular medium to refill the ER with Ca^{2+}. The same method was used to make $[Ca^{2+}]_M$ measurements in permeabilized cells, except for the facts that Ca^{2+} depletion prior reconstitution was not necessary and the final Ca^{2+} buffer perfused was 5.5 μM (Suppl. Fig. 1). Temperature was set at 37 °C during the experiments. Calibration of the luminescence data into $[Ca^{2+}]$ was made using an algorithm as previously described [21]. Statistical data are given as mean ± S.E.M.

Dorsomorphin was always added to the culture medium 48 h prior to the experiments. In the case of A769662, it was either added to the culture 48 h prior to the experiments or incubated with the cells for 2 h at 37 °C just before the experiments. This last method proved to be more effective to reach the maximum effect, and was also used for two other inhibitors, metformin and AICAR.

2.3. Measurement of ATP

Cellular ATP measurement was carried out using an ATP Colorimetric Assay Kit (MAK190, Sigma, Madrid), following the instructions of the supplier. Measurements were carried out in triplicate samples using a TECAN Genios Pro microplate reader (Tecan Austria GmbH, Salzburg, Austria).

2.4. Phospho-proteomics

2.4.1. Cell lysis and phosphopeptide enrichment

A769662, dorsomorphin and non-treated Hela cell lysis was carried out for 20 min at 4 °C in RIPA buffer containing broad spectrum kinase and phosphatase inhibitors (Roche, Madrid, Spain). After reduction and alkylation, proteins were precipitated, digested with an enzyme cocktail of trypsin/LysC (Promega, WI, USA) and the resulting peptides were isobarically labelled with Tandem Mass Tag 10plex™ (TMT-10-plex from Thermo Scientific, IL, USA). The differentially labeled samples were then pooled after reaction quenching with hydroxylamine and cleaned-up (Oasis HLB cartridges from Waters, MA, USA). The samples were finally dried and enriched for the phosphorylated peptides with TiO_2 Mag Sepharose magnetic beads (GE Healthcare, Glattbrugg, Switzerland) according to the manufacturer's instruction and analyzed with reversed-phase liquid chromatography tandem mass spectrometry

(RP-LC MS/MS). In parallel, non-phospho-enriched fractions (*i.e.*, 1/10 of the samples) were kept for complementary RP-LC MS/MS analysis.

2.4.2. Reversed-phase liquid chromatography tandem mass spectrometry

The samples (non-enriched and enriched fractions) were dissolved in H_2O/CH_3CN/formic acid 96.9/3/0.1 for RP-LC MS/MS analysis. RP-LC MS/MS was performed on an Orbitrap Fusion Lumos Tribrid mass spectrometer and an Ultimate 3000 RSLC nano system (Thermo Scientific, IL, USA) as previously described [22]. Proteolytic peptides were trapped on a PepMap 300 µm × 1 mm (C18, 5 µm, 100 Å) µ-pre-column, and separated on an Acclaim PepMap RSLC 75 µm × 50 cm (C18, 2 µm, 100 Å) column (Thermo Scientific, IL, USA) coupled to a stainless steel nanobore emitter (40 mm, OD 1/32") (Thermo Scientific, IL, USA). The column was heated to 50 °C using a PRSO-V1 column oven (Sonation, Biberach, Germany). Peptide separation was performed with a gradient of mobile phase A (H_2O/CH_3CN/FA 97.9/2/0.1) and B (H_2O/CH_3CN/FA 19.92/80/0.08): from 6.3% to 11% B over 12 min, from 11% to 25.5% B over 117 min and from 25.5% to 40% B over 28 min, with final elution (98% B) and equilibration (6.3% B) for a further 23 min. The flow rate was 220 nL·min^{-1} with a total analysis time of 180 min.

Data were acquired using a data-dependent method. A positive ion spray voltage of 1700 V and a transfer tube temperature of 275 °C were set up. For MS survey scans in profile mode, the Orbitrap resolution was 120,000 at $m/z = 200$ (automatic gain control (AGC) target of 2×10^5) with a m/z scan range from 300 to 1500, RF lens set at 30%, and maximum injection time of 100 ms. For MS/MS with higher-energy collisional dissociation (HCD) at 35% of the normalized collision energy, AGC target was set to 1×10^5 (isolation width of 0.7 in the quadrupole), with a resolution of 50,000 at $m/z = 200$, first mass at $m/z = 100$, and a maximum injection time of 86 ms with Orbitrap acquiring in profile mode. A duty cycle time of 3 s (top speed mode) was used to determine the number of precursor ions to be selected for HCD-based MS/MS. Ions were injected for all available parallelizable time. Dynamic exclusion was set for 60 s within a ± 10 ppm window. A lock mass of $m/z = 445.1200$ was used.

2.4.3. Mass spectrometry data processing

Protein identification was performed using Mascot 2.4.0 (Matrix Sciences, London, UK) against the human proteome database, UniProtKB (27/08/2014 release; 71,785 entries). Trypsin was selected as the proteolytic enzyme, with a maximum of two potential missed cleavages. Peptide and fragment ion tolerance were set to, respectively, 10 ppm and 0.02 Da. Fixed modifications included carbamidomethylation of cysteine TMT-labeling of lysine and TMT-labeling of peptide amino terminus. Variable modifications included oxidation of methionine, deamination of asparagine and glutamine, and phosphorylation of serine, threonine, and tyrosine. Mascot result files from both non-enriched and enriched fractions were loaded together into Scaffold Q + S 4.3.2 (Proteome Software, OR, USA) for normalization purposes and further searched with X! Tandem (The GPM, thegpm.org; version CYCLONE (2010.12.01.1)). Both peptide and protein false discovery rates were fixed at 1% maximum, with a one-unique-peptide criterion to report protein identification. Scaffold PTM 3.0.0 (Proteome Software) was used to annotate post-translational modifications from Scaffold results. Minimum localization probability was 95%. Isobaric tagging quantitative values for phosphorylated peptides were exported from Scaffold PTM and relative quantification of phosphorylation sites was computed using an in-house script with R version 3.1.1 (http://www.r-project.org/).

2.5. Materials

Coelenterazine wild-type and coelenterazine i were obtained from Biotium Inc., Hayward, Ca, U.S.A. A769662, dorsomorphin, ML-347, and DMH1 were from Tocris, Bristol, U.K. Inositol 1,4,5-trisphosphate was from Sigma, Madrid. Other reagents were from Sigma, Madrid, Spain or Merck, Darmstadt, Germany.

3. Results

3.1. Effect of AMPK modulators on histamine-induced cytosolic and mitochondrial [Ca^{2+}] peaks

We have studied the effects of the AMPK activator A769662 and the AMPK inhibitor dorsomorphin on intracellular Ca^{2+} signaling in HeLa cells. The human cervical cancer HeLa cell line has been widely used to study subcellular Ca^{2+} signaling after hormone stimulation. In fact, the first dynamic [Ca^{2+}] measurements inside mitochondria and endoplasmic reticulum were obtained in HeLa cells stimulated with histamine [23,24]. HeLa cells express endogenous histamine H1 G-protein coupled receptors that elicit a very strong response of IP_3 production followed by IP_3R activation and Ca^{2+} release from the ER [25]. Regarding the modulators, A769662 has been shown to activate AMPK by direct binding to the enzyme [26,27]. On the other hand, dorsomorphin (originally called Compound C) is a potent inhibitor of AMPK [28], although it has also been found to inhibit potently several bone morphogenetic protein type I receptors [29]. Both A769662 and dorsomorphin have been widely used in HeLa cells to activate or inhibit AMPK, and they have been described as effective AMPK modulators in these cells at the concentrations used in this paper [30–34].

Fig. 1a shows the effects of these compounds on the cytosolic [Ca^{2+}] peak induced by histamine. They induce opposite effects. A769662 reduces the height of the peak while dorsomorphin enhances it, and both effects were highly significant. Fig. 1b shows that the same effects were obtained in the absence of extracellular Ca^{2+}, that is, in the presence of EGTA in the extracellular medium. This means that these compounds act on IP_3-induced Ca^{2+}-release triggered by histamine and not on the store operated Ca^{2+} entry activated as a consequence of ER Ca^{2+} depletion. Fig. 1c shows the effects of these compounds on the mitochondrial Ca^{2+} uptake induced by histamine. During stimulated ER-Ca^{2+} release, mitochondria takes up Ca^{2+} from local high-Ca^{2+} microdomains generated in the cytosolic mouth of the IP_3R channels. This ER-mitochondria Ca^{2+} transfer occurs at MAMs, where both ER-IP_3R and mitochondrial MCU channels are placed [35]. This preferential Ca^{2+} pathway between both organelles allows mitochondria to sense and amplify the cytosolic [Ca^{2+}] signaling induced by Ca^{2+} release from the ER. Fig. 1c shows that the mitochondrial [Ca^{2+}] peak induced by histamine in control cells is much larger than the cytosolic one, around 20µM as previously reported [36]. Moreover, as a result of the amplification, the compounds A769662 and dorsomorphin produced also much larger effects, inhibition in the case of A769662 and activation in the case of dorsomorphin. A769662 inhibited the histamine-induced cytosolic [Ca^{2+}] peak by 16 ± 3%, but reduced the mitochondrial [Ca^{2+}] peak by 45 ± 3%. Similarly, dorsomorphin increased the histamine-induced cytosolic [Ca^{2+}] peak by 17 ± 2% and the mitochondrial one by 65 ± 6%.

These effects were obtained using a histamine concentration (100µM) that produces maximum IP_3 concentrations in these cells [25], but the same effects were obtained after submaximal stimulation (5µM histamine), that produces smaller and more physiological IP_3 concentrations (Supplementary Fig. 1A). We have also made several control experiments to exclude some alternative explanations of these effects. To test if the changes in mitochondrial Ca^{2+} uptake could be due to changes in the expression of the mitochondrial Ca^{2+} uniporter complex or changes in membrane potential, we measured the rate of mitochondrial Ca^{2+} uptake in permeabilized cells after addition of a controlled Ca^{2+} buffer. We found no changes in the rate of mitochondrial Ca^{2+} uptake among treated and untreated cells (Supplementary Fig. 1B). Control experiments also showed that the solvent added with the AMPK modulators (DMSO) had no effect by itself on the mitochondrial Ca^{2+} peak (Supplementary Fig. 1C). On the other hand,

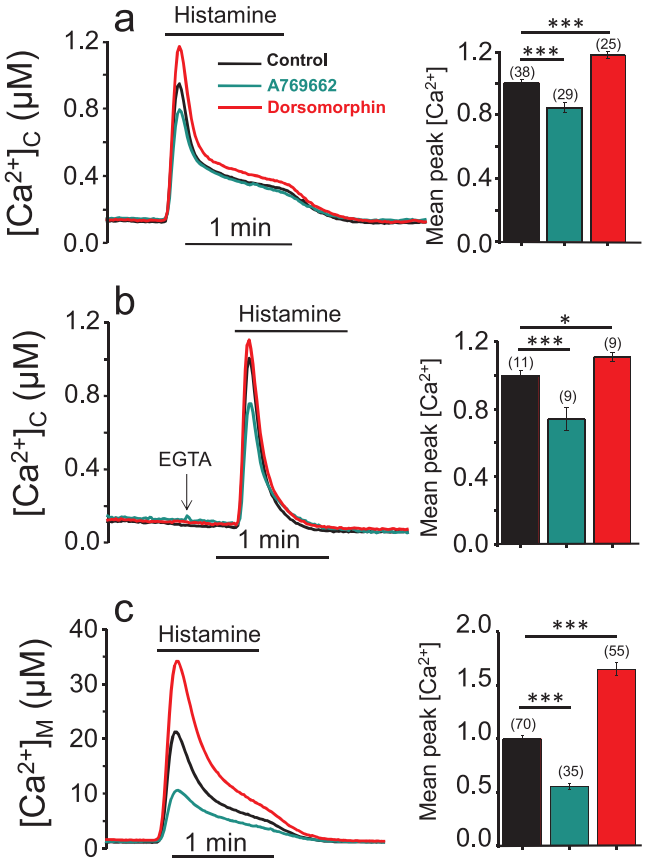

Fig. 1. Effects of A769662 and dorsomorphin on the cytosolic and mitochondrial [Ca^{2+}] peaks induced by histamine. HeLa cells were transfected with either cytosolic aequorin (panels a and b) or mitochondrially targeted mutated aequorin (panel c) and then cultured during 48 h with either none, 50μM A769662 or 1μM dorsomorphin. Then, cells were reconstituted with wild-type coelenterazine and stimulated with 100μM histamine as shown in the figure. In panel b, medium containing 0.5 mM EGTA instead of 1 mM Ca^{2+} was perfused when indicated. The right part of each panel shows the statistics of the [Ca^{2+}] peaks. The numbers on top of the bars are the number of experiments of each type. *, $p < 0.05$; ***, $p < 0.005$.

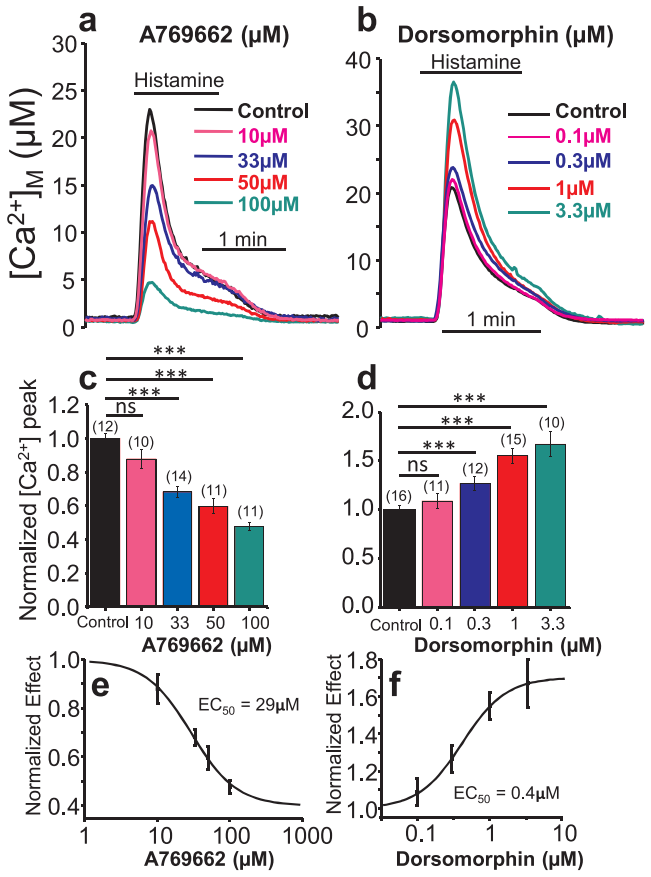

Fig. 2. Dose-response relationship of the effects of A769662 and dorsomorphin on the mitochondrial [Ca^{2+}] peaks induced by histamine. HeLa cells were transfected with mitochondrially targeted mutated aequorin and then cultured during 48 h with either none or different concentrations of dorsomorphin. In the case of A769662, cells were incubated with different concentrations of the compound for 2 h at 37 °C prior to the experiment. Then, cells were reconstituted with wild-type coelenterazine and stimulated with 100μM histamine as shown in panels a and b. Panels c and d show the statistics of the effects obtained in a series of experiments similar to those of panels a and b. The numbers on top of the bars are the number of experiments of each type. Panels e and f show the dose-response curve fitted to the experimental data and the EC50 obtained for each of the compounds. ***, $p < 0.005$.

AMPK activation should increase ATP concentration and ATP has been described to be an activator of the IP_3R [37]. This effect should produce activation of the IP_3R by the AMPK activator, while we find the opposite effect. We have anyway measured cellular ATP concentrations in the different conditions. The values obtained were (mean ± S.E.M., n = 3): Control (48 h with 0.02% DMSO), 19.3 ± 0.3 nmol/mg prot ; 48 h treatment with A769662, 20.8 ± 0.3 nmol/mg prot; 48 h treatment with dorsomorphin, 17.3 ± 1.0 nmol/mg prot. The differences observed were small and could not explain the effects of the modulators, as they would produce only minor changes in IP_3R activity in the opposite direction to that observed. We have also tested the effects of two other AMPK activators, metformin and AICAR. Supplementary Fig. 1D shows that they also reduced the mitochondrial [Ca^{2+}] peak induced by histamine, although the effect was much smaller than that induced by A768662. This is consistent with their mechanism of action (see Discussion below). Finally, the effect of AMPK-targeted shRNAs (PRKAA1 human shRNA plasmid kit, Origene, USA) was tested. Unfortunately, 48 h treatment with the scramble shRNA produced a large increase in the histamine-induced $[Ca^{2+}]_M$ peak, similar to that induced by dorsomorphin. No further effect was obtained with the AMPK-targeted shRNAs, perhaps because stimulation was already maximum.

Fig. 2 shows the dose-response curves for the effects of A769662 and dorsomorphin on the histamine-induced mitochondrial Ca^{2+} uptake. The amplification of the effects of these compounds on histamine-induced mitochondrial Ca^{2+} uptake provides a much better resolution of the effects at different concentrations of the drugs. The upper panels (a and b) show the effects of different concentrations of both compounds in a typical experiment. The middle panels (c and d) show the statistics of a series of experiments performed at each concentration, and the lower panels (e and f) show the dose response curves obtained. Half-maximal inhibition of the histamine-induced mitochondrial Ca^{2+} peak was obtained at 29μM A769662, and half-maximal activation was obtained at 0.4 μM dorsomorphin.

3.2. Effect of AMPK modulators on ER-Ca^{2+} release

The data of Figs. 1 and 2 show that A769662 and dorsomorphin induce the same effect (decrease for A769662 and increase for dorsomorphin) on both cytosolic and mitochondrial [Ca^{2+}] peaks induced by histamine. This suggests that both AMPK regulators influence calcium signaling at the level of ER Ca^{2+} release induced by histamine. Indeed, Fig. 3a shows that A769662 strongly inhibited the ER Ca^{2+} release induced by histamine, while dorsomorphin enhanced it. The statistics shows the mean values of the maximum $[Ca^{2+}]_{ER}$ decrease induced by histamine addition. A769662 largely inhibited Ca^{2+} release, while dorsomorphin produced the opposite effect.

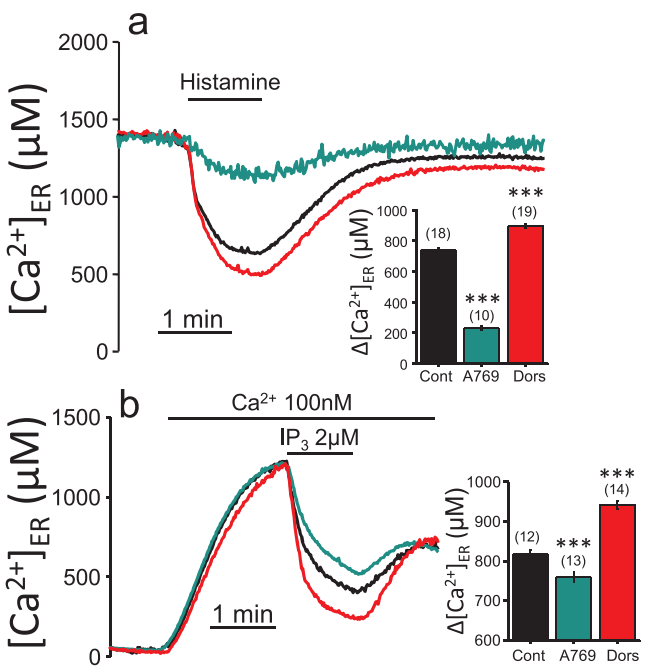

Fig. 3. Effects of A769662 and dorsomorphin on ER-Ca^{2+} release induced by histamine. HeLa cells were transfected with ER-targeted double-mutated aequorin and then cultured during 48 h with either none or 1μM dorsomorphin. In the case of A769662, cells were incubated with 100μM of the compound for 2 h at 37 °C prior to the experiment. In panel a, cells were reconstituted with coelenterazine i and then stimulated with 100μM histamine, as shown in the figure. In panel b, cells were permeabilized as described in Methods and reconstituted with coelenterazine wild-type. Then, as indicated in the figure, a 100 nM [Ca^{2+}] buffer was perfused to refill the ER followed by 2μM IP_3. The insets show the statistics of the effects obtained in a series of experiments similar to those of panels a and b. The numbers on top of the bars are the number of experiments of each type. ***, $p < 0.005$. The effect of each compound is compared with the control.

The effects of A769662 and dorsomorphin on histamine-induced ER Ca^{2+}-release suggest that these compounds influence IP_3R function, which is responsible for ER Ca^{2+} release triggered by histamine. However, we could still not exclude an effect of these compounds on the histamine receptor or the pathway responsible for IP_3 production after histamine action. We have then tested the effect of A769662 and dorsomorphin on ER Ca^{2+}-release induced directly by IP_3 in permeabilized cells. Fig. 3b shows that the same modulation can be obtained under these conditions. A769662 reduced IP_3-induced Ca^{2+} release and dorsomorphin enhanced it, confirming that the effect takes place directly at the IP_3R level. In conclusion, A769662 and dorsomorphin produce an opposite modulation of IP_3R activity, inhibition in the case of A769662 and activation in the case of dorsomorphin. Fig. 3b shows also that the rate of refilling with Ca^{2+} of the ER was not modified by these compounds.

3.3. Effect of BMPR inhibitors on histamine-induced cytosolic and mitochondrial [Ca^{2+}] peaks

Dorsomorphin, also called compound C, has been widely used as a selective AMPK inhibitor. However, it is also a potent inhibitor of bone morphogenetic protein type I receptors (BMPR) [29,38]. To exclude that the effect of dorsomorphin could be mediated by inhibition of BMPR, we have tested two different inhibitors of BMPR, which have no activity on AMPK (ML347 and DMH1). These compounds are even more potent inhibitors of BMPR than dorsomorphin [39], and were thus assayed at the same concentration. Fig. 4a and b, shows their effect on the cytosolic and mitochondrial [Ca^{2+}] peak induced by histamine.

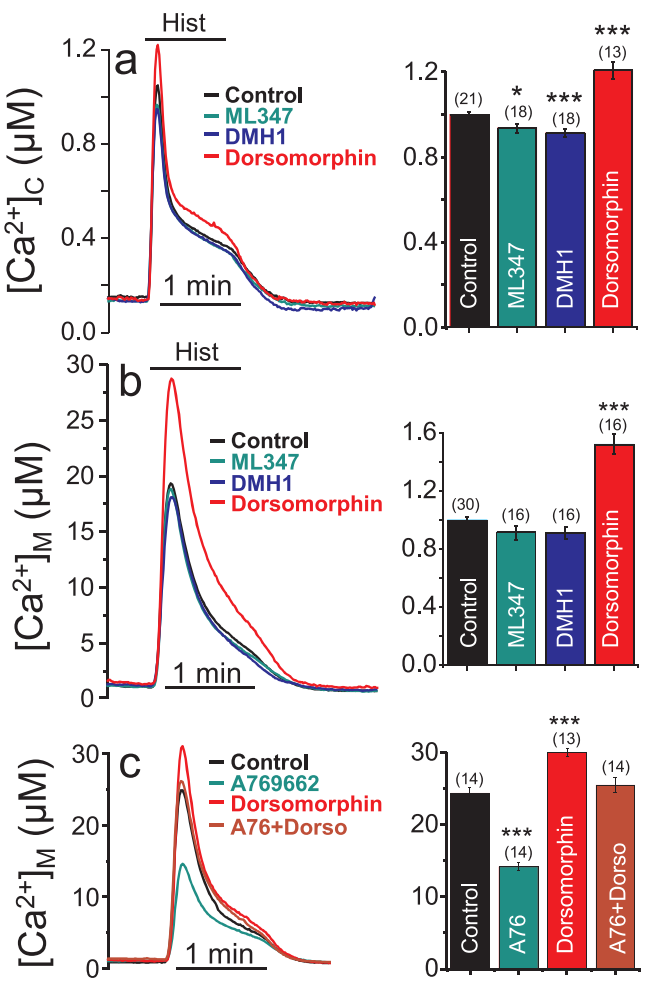

Fig. 4. Effects of the BMPR-inhibitors ML347 and DMH1 and of the AMPK/BMPR inhibitor dorsomorphin on the cytosolic and mitochondrial [Ca^{2+}] peaks induced by histamine. HeLa cells were transfected with either cytosolic aequorin (panel a) or mitochondrially targeted mutated aequorin (panels b and c) and then cultured during 48 h with either none, 1μM of ML347, DMH1 or dorsomorphin, or 50μM of A769662. Then, cells were reconstituted with wild-type coelenterazine and stimulated with 100μM histamine as shown in the figure. The right part of each panel shows the statistics of the [Ca^{2+}] peaks. The numbers on top of the bars are the number of experiments of each type. *, $p < 0.05$; ***, $p < 0.005$. The effect of each compound is compared with the control.

None of them increased the cytosolic or the mitochondrial [Ca^{2+}] peak. In fact, both produced significant reductions in the height of the cytosolic [Ca^{2+}] peak, in contrast with the very significant increase induced by dorsomorphin. Moreover, dorsomorphin reversed the inhibition of the histamine-induced mitochondrial [Ca^{2+}] peak induced by the AMPK activator A769662 (Fig. 4c). In conclusion, the effect of dorsomorphin on the IP_3R is not mediated by BMPR inhibition, but rather by AMPK inhibition.

3.4. Phosphoproteomic study

To obtain further insight on the mechanism of the effect of A769662 and dorsomorphin, we looked for changes in the protein phosphorylation state generated by the treatment with either A769662 or dorsomorphin. The comparative phosphoproteomic study reveals 304 P-sites with significant changes in phosphorylation induced by A769662 (Fig. 5A, Supplementary Table 1) and 257 P-sites having significant changes in phosphorylation induced by dorsomorphin (Fig. 5B, Supplementary Table 2). As we could not detect any significant changes in

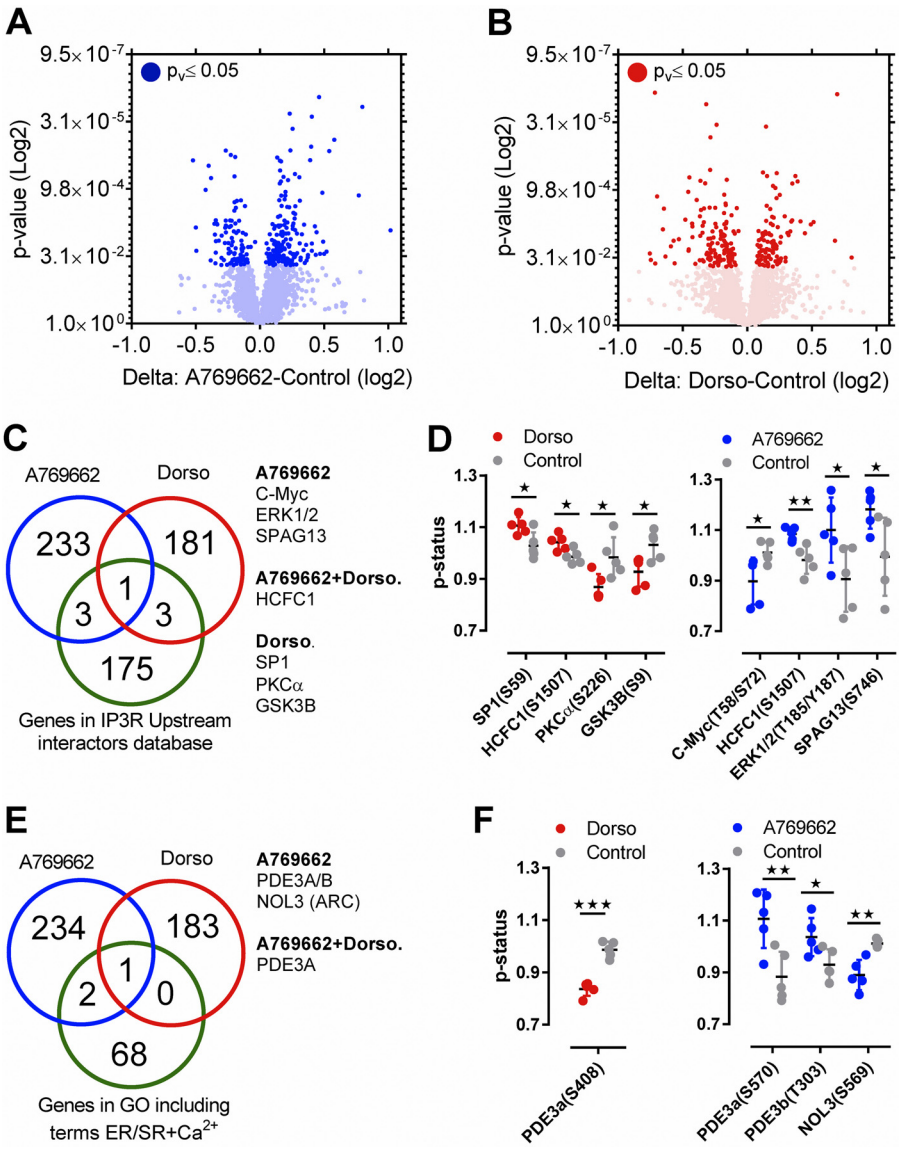

Fig. 5. Effects of AMPK modulators on Hela cells phospho-proteome. A) Volcano plot displaying significant regulated P-sites in presence of A769662. B) Volcano plot displaying significant regulated P-sites in presence of dorsomorphin. C) Identification of upstream IP_3R interactors significantly regulated in the presence of A769662 and Dorsomorphin (Venn diagram). The genes corresponding to the intersections are mentioned on the right, and panel D shows the magnitude of the changes in those genes. D) Left plot: effect of dorsomorphin on the phosphorylation status of SP1, HCFC1, PKCα and GSK. Right plot: effect of A769662 on the phosphorylation status of c-Myc, HCFC1, Erk1/2 and SPAG13 (p-status in lineal scale). E) Identification of genes belonging to gene ontologies including the terms: Endoplasmic reticulum / Sarcoplasmic reticulum and calcium, and significantly regulated in presence of A769662 and Dorsomorphin (Venn diagram). The genes corresponding to the intersections are mentioned on the right, and panel F shows the magnitude of the changes in those genes. F) Left plot: effect of dorsomorphin on the phosphorylation status of PDE3. Right plot: effect of A769662 on the phosphorylation status of PDE3a, PDE3b and NOL3 (p-status in lineal scale).

phosphorylation of the IP_3R itself, we tested for possible changes in the expression of IP_3R after incubation of cells with AMPK modulators. Supplementary Fig. 2 shows the mean level of the peptides obtained in the phosphoproteomic study from the two IP_3R isoforms present in the HeLa cells (3 peptides for type 1 (ITPR1) and 2 peptides for type 3 (ITPR3)). None of them experienced significant changes in expression after the treatments.

As we could not find changes in expression of phosphorylation of IP_3R, the effect of the AMPK modulators was probably indirect, mediated by an IP_3R upstream signaling pathway. Thus, we made a search for candidates to participate in this signaling pathway among the proteins that had shown significant changes in phosphorylation induced by the modulators. First, we found that several of these proteins belonged to the IP_3R interactome. Fig. 5C shows a Venn diagram listing the candidate genes resulting from this study and Fig. 5D shows the differences in phosphorylation status obtained for these genes (Additional data in Supplementary Fig. 3). This group included transcription factors such as c-Myc or SP1, the transcriptional regulator HCFC1, the small GTPase SPAG1 and several kinases, such as ERK1/2 (MAPK1/3), whose phosphorylation was increased by A769662, and PKCα and GSK3B, whose phosphorylation was decreased in the presence of dorsomorphin.

In addition, a Gene Ontology study was performed applying Metacore (Thompson Reuters) to reveal proteins related to Ca^{2+}-signaling which become phospho-regulated in the presence of A769662 or dorsomorphin. Supplementary table 3 shows the full list of proteins obtained under these conditions, classified according to their participation in different calcium signaling pathways. Some of them are directly related with the regulation of Ca^{2+} release from the endoplasmic/sarcoplasmic reticulum. Fig. 5E shows a Venn diagram listing the candidate genes that meet these conditions and Fig. 5F shows the differences in phosphorylation status obtained for these genes. Among them, it is worth to mention the phospho-regulation of phosphodiesterase 3 A (PDE3 A), which becomes phosphorylated in the presence of A769662 (1.2534 fold, S570) and dephosphorylates in the presence of dorsomorphin (0.84 fold, S408) (Fig. 5E). PDE3b is also phosphorylated in the presence of A769662, and the group also includes the Ca^{2+}-dependent apoptosis inhibitor NOL3 (ARC), whose phosphorylation decreases in the presence of A769662.

4. Discussion

The relationship between AMPK regulation and Ca^{2+} signaling is still unclear. We have investigated here the effects of the AMPK activator A769662 and the AMPK inhibitor dorsomorphin on subcellular Ca^{2+} signaling in HeLa cells. Our results show that A769662 and dorsomorphin have a clear and opposite effect on IP_3-induced ER Ca^{2+}

release. The AMPK activator inhibited IP_3-induced ER Ca^{2+} release and the AMPK inhibitor activated it. In both cases, the effects were large enough to produce highly significant changes in the histamine-induced cytosolic and mitochondrial [Ca^{2+}] peaks. In particular, the Ca^{2+} transfer between ER and mitochondria was specially affected, as the AMPK modulators dramatically modified agonist-induced mitochondrial [Ca^{2+}] increase. Our data indicate that the AMPK modulators directly influence IP_3R activity, as they produced similar effects on histamine-induced Ca^{2+} release in intact cells and on IP_3-induced Ca^{2+} release in permeabilized cells. However, the resting $[Ca^{2+}]_{ER}$ was not modified, indicating that the compounds only modulate the response of the IP_3R to IP_3, and have no direct effect in the absence of IP_3.

A769662 is a direct activator of AMPK which stimulates its activity even in the absence of AMPK phosphorylation [40]. The EC50 for inhibition by A769662 of IP_3-induced Ca^{2+} release was 29μM, a concentration in the same range as previously determined to activate AMPK in HeLa cells [30,31]. The smaller effect of metformin and AICAR is consistent [30,40] with the fact that A769662 is a direct activator of AMPK, while metformin and AICAR are indirect activators of AMPK that induce its phosphorylation by either LKB1 kinase (absent in HeLa cells) or CaMKKβ. In fact, it has been reported before that A769662 is a much better AMPK activator in HeLa cells than metformin or AICAR [31]. Regarding dorsomorphin/Compound C, it was originally identified as an inhibitor of AMPK and it has been widely used as an AMPK inhibitor in HeLa cells [32–34]. However, it has been found that it is also a potent inhibitor of several BMPR [38]. In our work, the EC50 for stimulation by dorsomorphin of the histamine-induced $[Ca^{2+}]_M$ peak was very low, only 0.4μM, compatible with a specific effect either on AMPK or BMPR. To distinguish between these two possibilities, we have assayed the effect on Ca^{2+} homeostasis of two different BMPR inhibitors which have no effect on AMPK. Our data show that these inhibitors did not reproduce at all the effects of dorsomorphin on the cytosolic and mitochondrial [Ca^{2+}] peaks induced by histamine, suggesting that the effect of dorsomorphin shown here is not due to BMPR inhibition. Moreover, dorsomorphin reversed the effects of the AMPK activator A769662 on the histamine-induced $[Ca^{2+}]_M$ peaks, suggesting that its effects are actually due to AMPK inhibition.

The observed effect of the modulators is consistent with the well-known effects of AMPK on metabolism and with the general antagonism between AMPK and mTOR activation. We find that an AMPK activator inhibits IP_3-induced Ca^{2+} release, while an AMPK inhibitor activates it. As Ca^{2+} is a key second messenger for cell activation, inhibition of Ca^{2+} release should slow down energy consumption for different Ca^{2+}-dependent activities such as contraction, secretion, proliferation, and others. In addition, less energy would be required to restore the Ca^{2+} gradients via ATP-dependent Ca^{2+} pumps. Therefore, inhibition of IP_3R may reduce energy expenditure. Furthermore, inhibition of IP_3R should also reduce Ca^{2+} transfer from ER to mitochondria, and this should slow down ATP production. This apparent contradiction adds to some other uncertainties that remain on the relationship between nutrient-sensitive pathways and Ca^{2+} signaling. As we have mentioned before, mTOR has been reported to induce both activation [12–14] and inhibition [11] of IP_3R. Similarly, the regulation of autophagy by Ca^{2+}, involving AMPK and mTOR as active players, is highly controversial. While considerable evidence suggests that cytosolic Ca^{2+} favors autophagy, under some conditions it seems to have the ability to block it as well [41].

We would like to highlight that IP_3R-induced Ca^{2+} transfer from ER to mitochondria has been shown to be essential to maintain mitochondrial function and cellular energy balance not only in normal cells, but especially in cancer cells. Genetic or pharmacological inhibition of IP_3R produces cell death with much greater potency in cancer cells than in normal cells, and IP_3R seems to play an important role in cancer progression and metastasis (see [42] for a review). Under this perspective, the regulation of IP_3R by AMPK described here may be of interest for cancer research.

The mechanism linking AMPK regulation to ER Ca^{2+} release will require further studies. In order to obtain some additional information on the possible mechanisms, we performed a phosphoproteomic study looking for changes in protein phosphorylation induced by treatment with these compounds. This study showed that A769662 and dorsomorphin generate a large amount of changes in the protein phosphorylation pattern. In the case of A769662, the phosphorylated proteins include several targets of AMPK, such as acetyl-CoA carboxylase or Raf, consistent with activation of AMPK in the presence of this compound. However, the large number of protein phosphorylation changes makes it difficult to define clearly the mechanisms involved.

Analysis of the phosphoproteomic data suggests several possible candidates to mediate the effects, although much further work is required to test it. First, several kinases which are upstream of the IP_3R in the interactome become phosphorylated or dephosphorylated in the presence of these compounds. They are ERK1/2 (MAPK1/3), whose phosphorylation was increased by A769662, and PKCα and GSK3B, whose phosphorylation was decreased in the presence of dorsomorphin. Both ERK1/2 and PKC have been shown to phosphorylate IP_3R [43]. In addition, we should mention the phosphodiesterase PDE3 A, which becomes phosphorylated in the presence of A769662 and dephosphorylates in the presence of dorsomorphin. PDE3 A (as well as PDE3B, which also becomes phosphorylated in the presence of A769662) has been found associated with the endoplasmic reticulum [44] and cAMP is an important activator of the IP_3R, both directly and via PKA-mediated phosphorylation [45]. Activation of PDE in the presence of A769662 could therefore reduce the cAMP concentration (from the resting levels, see [46,47]) and thereby inhibit the IP_3R. In fact, it has been shown that a closely related phosphodiesterase, PDE4B, is phosphorylated by AMPK at three sites [48]. Finally, we should mention the Ca^{2+}-dependent apoptosis inhibitor NOL3 (ARC), whose phosphorylation decreases in the presence of A769662 (Fig. 5F). It may also be an interesting candidate, as it has been shown to regulate Ca^{2+}-release from sarcoplasmic reticulum [49].

5. Conclusions

Our data suggest that AMPK negatively regulates IP_3-induced Ca^{2+} release from the ER, although further studies are required to investigate the mechanism of this effect. This modulation reinforces the link between Ca^{2+} signaling and the AMPK pathway and places the IP_3R, also regulated by mTOR, as a key signaling hub for these two major nutrient-sensitive pathways.

Author contributions

JAdV performed most of the Ca^{2+} experiments, and PG-C and PA-I joined in performing some of them. ANG and JS-D performed the phosphoproteomic experiments and JS-D analyzed it. JA wrote the manuscript and ANG, JS-D, AW, RIF and MM helped in discussing and editing the manuscript. All authors have read and approved the final manuscript.

Conflict of interest

The authors declare that there are no conflicts of interest.

Acknowledgements

This work was supported by grants from the Spanish Ministerio de Economía y Competitividad [BFU2014-55731-R and BFU2017-83509-R], projects co-financed by the European Union through the European Regional Development Fund. JA-d-V has a fellowship from Junta de Castilla y León (JCyL), cofinanced by the Fondo Social Europeo (FSE). PG-C has a FPI fellowship from Ministerio de Economía y Competitividad. We also thank Löic Dayon (NIHS) for his support to

address the phospho-proteomic experiment.

Appendix A. Supplementary data

Supplementary material related to this article can be found, in the online version, at doi:https://doi.org/10.1016/j.ceca.2018.12.004.

References

[1] S.C. Lin, D.G. Hardie, AMPK: sensing glucose as well as cellular energy status, Cell Metab. 27 (2018) 299–313, https://doi.org/10.1016/j.cmet.2017.10.009.

[2] W.W. Winder, D.G. Hardie, AMP-activated protein kinase, a metabolic master switch: possible roles in type 2 diabetes, Am. J. Physiol. 277 (1999) E1–10, https://doi.org/10.1152/ajpendo.1999.277.1.E1.

[3] C. Lopez-Otin, L. Galluzzi, J.M.P. Freije, F. Madeo, G. Kroemer, Metabolic control of longevity, Cell 166 (2016) 802–821, https://doi.org/10.1016/j.cell.2016.07.031.

[4] C.E. Riera, C. Merkwirth, C.D. De Magalhaes Filho, A. Dillin, Signaling networks determining life span, Annu. Rev. Biochem. 85 (2016) 35–64, https://doi.org/10.1146/annurev-biochem-060815-014451.

[5] A. Woods, K. Dickerson, R. Heath, S.P. Hong, M. Momcilovic, S.R. Johnstone, M. Carlson, D. Carling, Ca^{2+}/calmodulin-dependent protein kinase kinase-beta acts upstream of AMP-activated protein kinase in mammalian cells, Cell Metab. 2 (2005) 21–33, https://doi.org/10.1016/j.cmet.2005.06.005.

[6] S.M. Jeon, Regulation and function of AMPK in physiology and diseases, Exp. Mol. Med. 48 (2016) e245, https://doi.org/10.1038/emm.2016.81.

[7] J.P. Decuypere, R.C. Paudel, J. Parys, G. Bultynck, Intracellular Ca^{2+} signaling: a novel player in the canonical mTOR-controlled autophagy pathway, Commun. Integr. Biol. 6 (2013), https://doi.org/10.4161/cib.25429 e25429.

[8] C. Cardenas, J.K. Foskett, Mitochondrial Ca^{2+} signals in autophagy, Cell Calcium 52 (2012) 44–51, https://doi.org/10.1016/j.ceca.2012.03.001.

[9] P. Gulati, L.D. Gaspers, S.G. Dann, M. Joaquin, T. Nobukuni, F. Natt, S.C. Kozma, A.P. Thomas, G. Thomas, Amino acids activate mTOR complex 1 via Ca^{2+}/CaM signaling to hVps34, Cell Metab. 7 (2008) 456–465, https://doi.org/10.1016/j.cmet.2008.03.002.

[10] N. Ito, U.T. Ruegg, A. Kudo, Y. Miyagoe-Suzuki, S. Takeda, Activation of calcium signaling through Trpv1 by nNOS and peroxynitrite as a key trigger of skeletal muscle hypertrophy, Nat Med. 19 (2013) 101–106, https://doi.org/10.1038/nm.3019.

[11] C. Betz, D. Stracka, C. Prescianotto-Baschong, M. Frieden, N. Demaurex, M.N. Hall, Feature article: mTOR complex 2-Akt signaling at mitochondria-associated endoplasmic reticulum membranes (MAM) regulates mitochondrial physiology, Proc. Natl. Acad. Sci. U. S. A. 110 (2013) 12526–12534, https://doi.org/10.1073/pnas.1302455110.

[12] D. MacMillan, S. Currie, K.N. Bradley, T.C. Muir, J.G. McCarron, In smooth muscle, FK506-binding protein modulates IP3 receptor-evoked Ca^{2+} release by mTOR and calcineurin, J. Cell Sci. 118 (2005) 5443–5451, https://doi.org/10.1242/jcs.02657.

[13] M.O. Fregeau, Y. Regimbald-Dumas, G. Guillemette, Positive regulation of inositol 1,4,5-trisphosphate-induced Ca^{2+} release by mammalian target of rapamycin (mTOR) in RINm5F cells, J. Cell Biochem. 112 (2011) 723–733, https://doi.org/10.1002/jcb.23006.

[14] Y. Regimbald-Dumas, M.O. Fregeau, G. Guillemette, Mammalian target of rapamycin (mTOR) phosphorylates inositol 1,4,5-trisphosphate receptor type 2 and increases its Ca^{2+} release activity, Cell Signal. 23 (2011) 71–79, https://doi.org/10.1016/j.cellsig.2010.08.005.

[15] J.B. Parys, J.P. Decuypere, G. Bultynck, Role of the inositol 1,4,5-trisphosphate receptor/Ca^{2+}-release channel in autophagy, Cell Commun. Signal. 10 (2012) 17, https://doi.org/10.1186/1478-811x-10-17.

[16] C. Cardenas, M. Muller, A. McNeal, A. Lovy, F. Jana, G. Bustos, F. Urra, N. Smith, J. Molgo, J.A. Diehl, T.W. Ridky, J.K. Foskett, Selective vulnerability of cancer cells by inhibition of Ca^{2+} transfer from endoplasmic reticulum to mitochondria, Cell Rep. 14 (2016) 2313–2324, https://doi.org/10.1016/j.celrep.2016.02.030.

[17] A. Ogawa, A.L. Firth, K.A. Smith, M.V. Maliakal, J.X. Yuan, PDGF enhances store-operated Ca^{2+} entry by upregulating STIM1/Orai1 via activation of Akt/mTOR in human pulmonary arterial smooth muscle cells, Am. J. Physiol. Cell Physiol. 302 (2012) C405–11, https://doi.org/10.1152/ajpcell.00337.2011.

[18] M. Montero, M.T. Alonso, E. Carnicero, I. Cuchillo-Ibanez, A. Albillos, A.G. Garcia, J. Garcia-Sancho, J. Alvarez, Chromaffin-cell stimulation triggers fast millimolar mitochondrial Ca^{2+} transients that modulate secretion, Nat. Cell Biol. 2 (2000) 57–61, https://doi.org/10.1038/35000001.

[19] S. de la Fuente, R.I. Fonteriz, P.J. de la Cruz, M. Montero, J. Alvarez, Mitochondrial free [Ca^{2+}] dynamics measured with a novel low-Ca^{2+} affinity aequorin probe, Biochem. J. 445 (2012) 371–376, https://doi.org/10.1042/BJ20120423.

[20] S. de la Fuente, R.I. Fonteriz, M. Montero, J. Alvarez, Ca^{2+} homeostasis in the endoplasmic reticulum measured with a new low-Ca^{2+}-affinity targeted aequorin, Cell Calcium 54 (2013) 37–45, https://doi.org/10.1016/j.ceca.2013.04.001.

[21] M. Montero, C.D. Lobaton, A. Moreno, J. Alvarez, A novel regulatory mechanism of the mitochondrial Ca^{2+} uniporter revealed by the p38 mitogen-activated protein kinase inhibitor sb202190, FASEB J. 16 (2002) 1955–1957, https://doi.org/10.1096/fj.02-0553fje.

[22] J. Lan, A. Nunez Galindo, J. Doecke, C. Fowler, R.N. Martins, S.R. Rainey-Smith, O. Cominetti, L. Dayon, A systematic evaluation of the use of human plasma and serum for mass spectrometry-based shotgun proteomics, J. Proteome Res. 17 (2018) 1426–1435, https://doi.org/10.1021/acs.jproteome.7b00788.

[23] R. Rizzuto, A.W.M. Simpson, M. Brini, T. Pozzan, Rapid changes of mitochondrial Ca^{2+} revealed by specifically targeted recombinant aequorin, Nature 358 (1992) 325–327, https://doi.org/10.1038/358325a0.

[24] M. Montero, M.J. Barrero, J. Alvarez, [Ca^{2+}] microdomains control agonist-induced Ca2+ release in intact HeLa cells, FASEB J. 11 (1997) 881–885, https://doi.org/10.1096/fasebj.11.11.9285486.

[25] B.C. Tilly, L.G. Tertoolen, A.C. Lambrechts, R. Remorie, S.W. de Laat, W.H. Moolenaar, Histamine-H1-receptor-mediated phosphoinositide hydrolysis, Ca^{2+} signalling and membrane-potential oscillations in human HeLa carcinoma cells, Biochem. J. 266 (1990) 235–243, https://doi.org/10.1042/bj2660235.

[26] R.G. Kurumbail, M.F. Calabrese, Structure and regulation of AMPK, in: M.D. Cordero, B. Viollet (Eds.), AMP-Activated Protein Kinase, Springer International Publishing, Cham, 2016, pp. 3–22, , https://doi.org/10.1007/978-3-319-43589-3_1.

[27] B. Guigas, B. Viollet, Targeting AMPK: from ancient drugs to New small-molecule activators, in: M.D. Cordero, B. Viollet (Eds.), AMP-Activated Protein Kinase, Springer International Publishing, Cham, 2016, pp. 327–350, , https://doi.org/10.1007/978-3-319-43589-3_13.

[28] G. Zhou, R. Myers, Y. Li, Y. Chen, X. Shen, J. Fenyk-Melody, M. Wu, J. Ventre, T. Doebber, N. Fujii, N. Musi, M.F. Hirshman, L.J. Goodyear, D.E. Moller, Role of AMP-activated protein kinase in mechanism of metformin action, J. Clin. Invest. 108 (2001) 1167–1174, https://doi.org/10.1172/jci13505.

[29] P.B. Yu, C.C. Hong, C. Sachidanandan, J.L. Babitt, D.Y. Deng, S.A. Hoyng, H.Y. Lin, K.D. Bloch, R.T. Peterson, Dorsomorphin inhibits BMP signals required for embryogenesis and iron metabolism, Nat. Chem. Biol. 4 (2008) 33–41, https://doi.org/10.1038/nchembio.2007.54.

[30] O. Goransson, A. McBride, S.A. Hawley, F.A. Ross, N. Shpiro, M. Foretz, B. Viollet, D.G. Hardie, K. Sakamoto, Mechanism of action of A-769662, a valuable tool for activation of AMP-activated protein kinase, J. Biol. Chem. 282 (2007) 32549–32560, https://doi.org/10.1074/jbc.M706536200.

[31] Y. Konagaya, K. Terai, Y. Hirao, K. Takakura, M. Imajo, Y. Kamioka, N. Sasaoka, A. Kakizuka, K. Sumiyama, T. Asano, M. Matsuda, A highly sensitive FRET biosensor for AMPK exhibits heterogeneous AMPK responses among cells and organs, Cell Rep. 21 (2017) 2628–2638, https://doi.org/10.1016/j.celrep.2017.10.113.

[32] L. Ting, W. Bo, R. Li, X. Chen, Y. Wang, Z. Jun, L. Yu, AMP-activated protein kinase supports the NGF-induced viability of human HeLa cells to glucose starvation, Mol. Biol. Rep. 37 (2010) 2593–2598, https://doi.org/10.1007/s11033-009-9780-3.

[33] I.J. Lee, C.W. Lee, J.H. Lee, CaMKKbeta-AMPKalpha2 signaling contributes to mitotic golgi fragmentation and the G2/M transition in mammalian cells, Cell Cycle 14 (2015) 598–611, https://doi.org/10.4161/15384101.2014.991557.

[34] B.Y.K. Law, F. Gordillo-Martinez, Y.Q. Qu, N. Zhang, S.W. Xu, P.S. Coghi, S.W.F. Mok, J. Guo, W. Zhang, E.L.H. Leung, X.X. Fan, A.G. Wu, W.K. Chan, X.J. Yao, J.R. Wang, L. Liu, V.K.W. Wong, Thalidezine, a novel AMPK activator, eliminates apoptosis-resistant cancer cells through energy-mediated autophagic cell death, Oncotarget 8 (2017) 30077–30091, https://doi.org/10.18632/oncotarget.15616.

[35] R. Filadi, P. Theurey, P. Pizzo, The endoplasmic reticulum-mitochondria coupling in health and disease: molecules, functions and significance, Cell Calcium 62 (2017) 1–15, https://doi.org/10.1016/j.ceca.2017.01.003.

[36] R.I. Fonteriz, S. de la Fuente, A. Moreno, C.D. Lobaton, M. Montero, J. Alvarez, Monitoring mitochondrial [Ca^{2+}] dynamics with rhod-2, ratiometric pericam and aequorin, Cell Calcium 48 (2010) 61–69, https://doi.org/10.1016/j.ceca.2010.07.001.

[37] D.O. Mak, S. McBride, J.K. Foskett, ATP regulation of type 1 inositol 1,4,5-trisphosphate receptor channel gating by allosteric tuning of Ca^{2+} activation, J. Biol. Chem. 274 (1999) 22231–22237, https://doi.org/10.1074/jbc.274.32.22231.

[38] C.C. Hong, P.B. Yu, Applications of small molecule BMP inhibitors in physiology and disease, Cytokine Growth Factor Rev. 20 (2009) 409–418, https://doi.org/10.1016/j.cytogfr.2009.10.021.

[39] D.W. Engers, A.Y. Frist, C.W. Lindsley, C.C. Hong, C.R. Hopkins, Synthesis and structure-activity relationships of a novel and selective bone morphogenetic protein receptor (BMP) inhibitor derived from the pyrazolo[1.5-a]pyrimidine scaffold of dorsomorphin: the discovery of ML347 as an ALK2 versus ALK3 selective MLPCN, Bioorg. Med. Chem. Lett. 23 (2013) 3248–3252, https://doi.org/10.1016/j.bmcl.2013.03.113.

[40] J.W. Scott, N. Ling, S.M. Issa, T.A. Dite, M.T. O'Brien, Z.P. Chen, S. Galic, C.G. Langendorf, G.R. Steinberg, B.E. Kemp, J.S. Oakhill, Small molecule drug A-769662 and AMP synergistically activate naive AMPK independent of upstream kinase signaling, Chem. Biol. 21 (2014) 619–627, https://doi.org/10.1016/j.chembiol.2014.03.006.

[41] M.D. Bootman, T. Chehab, G. Bultynck, J.B. Parys, K. Rietdorf, The regulation of autophagy by calcium signals: do we have a consensus? Cell Calcium 70 (2018) 32–46, https://doi.org/10.1016/j.ceca.2017.08.005.

[42] G. Bustos, P. Cruz, A. Lovy, C. Cárdenas, Endoplasmic reticulum–mitochondria calcium communication and the regulation of mitochondrial metabolism in cancer: a novel potential target, Front. Oncol. 7 (2017) 199, https://doi.org/10.3389/fonc.2017.00199.

[43] V. Vanderheyden, B. Devogelaere, L. Missiaen, H. De Smedt, G. Bultynck, J.B. Parys, Regulation of inositol 1,4,5-trisphosphate-induced Ca^{2+} release by reversible phosphorylation and dephosphorylation, Biochim. Biophys. Acta 1793 (2009) 959–970, https://doi.org/10.1016/j.bbamcr.2008.12.003.

[44] D.H. Maurice, H. Ke, F. Ahmad, Y. Wang, J. Chung, V.C. Manganiello, Advances in targeting cyclic nucleotide phosphodiesterases, Nat. Rev. Drug Discov. 13 (2014) 290–314, https://doi.org/10.1038/nrd4228.

[45] C.W. Taylor, Regulation of IP3 receptors by cyclic AMP, Cell Calcium 63 (2017) 48–52, https://doi.org/10.1016/j.ceca.2016.10.005.

[46] K. Harada, M. Ito, X. Wang, M. Tanaka, D. Wongso, A. Konno, H. Hirai, H. Hirase, T. Tsuboi, T. Kitaguchi, Red fluorescent protein-based cAMP indicator applicable to optogenetics and in vivo imaging, Sci. Rep. 7 (2017) 7351, https://doi.org/10.1038/s41598-017-07820-6.

[47] S. Borner, F. Schwede, A. Schlipp, F. Berisha, D. Calebiro, M.J. Lohse, V.O. Nikolaev, FRET measurements of intracellular cAMP concentrations and cAMP analog permeability in intact cells, Nat. Protoc. 6 (2011) 427–438, https://doi.org/10.1038/nprot.2010.198.

[48] M. Johanns, Y.C. Lai, M.F. Hsu, R. Jacobs, D. Vertommen, J. Van Sande, J.E. Dumont, A. Woods, D. Carling, L. Hue, B. Viollet, M. Foretz, M.H. Rider, AMPK antagonizes hepatic glucagon-stimulated cyclic AMP signalling via phosphorylation-induced activation of cyclic nucleotide phosphodiesterase 4B, Nat. Commun. 7 (2016) 10856, https://doi.org/10.1038/ncomms10856.

[49] D. Lu, J. Liu, J. Jiao, B. Long, Q. Li, W. Tan, P. Li, Transcription factor Foxo3a prevents apoptosis by regulating calcium through the apoptosis repressor with caspase recruitment domain, J. Biol. Chem. 288 (2013) 8491–8504, https://doi.org/10.1074/jbc.M112.442061.